Pairing Instabilities of the Extended Hubbard Model for Cu-O–Based Superconductors

P. B. Littlewood and C. M. Varma
AT&T Bell Laboratories, Murray Hill, New Jersey 07974

E. Abrahams
Serin Physics Laboratory, Rutgers University, Piscataway, New Jersey 08855

(Received 26 July 1989)

We use weak-coupling methods to calculate the effective interaction between quasiparticles induced by charge and spin fluctuations in a three-band model for the copper-oxide superconductors with both intersite and intrasite repulsion. The instabilities to superconducting states of different symmetries are calculated; besides the *d*-wave superconductivity near the antiferromagnetic instability, we find that extended *s*-wave superconductivity is favored by a charge-transfer resonance close to a valence instability. A phase diagram similar to experiments is obtained.

PACS numbers: 74.65.+n

It is a common feature of conventional superconductors that the transition temperature is raised by the proximity to a structural instability. Equally, it is expected that electronically driven superconductivity will be enhanced close to a magnetic or charge fluctuation instability, because there will be present low-energy fluctuations which enhance the effective interactions. In a three-band model with on-site and nearest-neighbor Coulomb interactions,[1] there are at least three instabilities which can be important. These are the spin-density-wave (SDW, or antiferromagnet) and charge-density-wave (CDW) instabilities, driven by *intra*band processes, and the charge-transfer instability (CTI) driven by *inter*band coupling induced by the Cu-O interaction. Close to half filling, and for nearly perfect nesting, either the SDW or CDW will dominate, depending on parameters. However, for larger values of the doping, it was found that the dominant charge-fluctuation instability was the CTI, which corresponds to a valence instability of the Cu and O charge.

In an earlier paper,[1] we calculated the charge and spin fluctuations in a three-band model for a two-dimensional square CuO_2 plane. In the present paper we calculate the effective particle-particle interaction and examine the question of superconductivity in the weak-coupling limit.

We use a Hamiltonian for the CuO_2 planes in a tight-binding basis which is an extended Hubbard model defined on the $d_{x^2-y^2}$ orbital for Cu and the $(\sigma)p_x$ orbital on one of the two O atoms in the unit cell and the $(\sigma)p_y$ orbital on the other:[2]

$$H=\epsilon\sum_i (c_{di}^\dagger c_{di}-c_{xi}^\dagger c_{xi}-c_{yi}^\dagger c_{yi})+\sum_{\langle ij\rangle}(t_{ij}c_{di}^\dagger c_{xj}+\text{H.c.}+x\rightarrow y)+\sum_{\langle ij\rangle}(t_{ij}'c_{xi}^\dagger c_{yj}+\text{H.c.})$$
$$+\tfrac{1}{2}U\sum_i \delta n_{di}\delta n_{di}+\tfrac{1}{2}U_p\sum_i(\delta n_{xi}\delta n_{xi}+x\rightarrow y)+V\sum_{\langle ij\rangle}\delta n_{di}(\delta n_{xj}+\delta n_{yj})\,. \quad (1)$$

Here $\epsilon=\frac{1}{2}(E_d-E_p)$, $t_{ij}=\pm t=\pm 1$, and we have included a repulsive U on Cu and O as well as the nearest-neighbor repulsive V. The notation $\langle ij\rangle$ specifies nearest-neighbor summation; t is the direct Cu-O overlap and t' is the nearest-neighbor O-O overlap. The band parameters ϵ and t include the Hartree-Fock renormalizations, and $\delta n_i=n_i-\langle n_i\rangle$. Holding ϵ fixed while varying n, U, V, etc. (as we shall do) requires that the "bare" E_d-E_p must also be changed. The band filling is written as $n=\frac{1}{2}(1-\delta)$, so that δ is the hole concentration. This model has been studied already by several techniques.[3]

We begin[1] by solving for the particle-hole T matrix from the Bethe-Salpeter equation, which leads to an effective interaction of a form factorizable[4] in terms of particle-hole basis functions g^i:

$$V_{\text{eff}}(\sigma_1\alpha\mathbf{k}+\mathbf{q};\sigma_2\beta\mathbf{k};\sigma_3\beta'\mathbf{k}';\sigma_4\alpha'\mathbf{k}'+\mathbf{q})=\sum_{ij} g_{\alpha\beta}^i(\mathbf{k},\mathbf{k}+\mathbf{q})g_{\alpha'\beta'}^j(\mathbf{k}',\mathbf{k}'+\mathbf{q})[\Gamma_\rho^{ij}(\mathbf{q},\omega)\delta_{1,2}\delta_{3,4}+\Gamma_s^{ij}(\mathbf{q},\omega)\boldsymbol{\sigma}_{1,2}\cdot\boldsymbol{\sigma}_{3,4}]\,, \quad (2)$$

Here $\alpha,\beta,\ldots$, refer to orbitals and the subscripts in numerals are spin indices. The kernel of the interaction term of Eq. (2) results from the solution of the matrix equations

$$\Gamma_{\rho,s}=[1-2v_{\rho,s}P]^{-1}v_{\rho,s}\,, \quad (3)$$

where $v_{\rho,s}^{ij}(\mathbf{q})$ are the bare interactions, and $P^{ij}(\mathbf{q},\omega)$ is the particle-hole polarizability in the basis of the g's. We have suppressed the indices and q $[=(\mathbf{q},\omega)]$ dependence for clarity.

We now take a conventional approach to study the superconducting transition by using the effective interaction V_{eff}, Eq. (2), as the bare interaction in the particle-particle channel. Solution of the particle-particle T-matrix equation leads to the equation for the gap function $\phi(p)$ at T_c,

$$\phi(\mathbf{p},\omega_n)=T_c\sum_{\mathbf{k}\nu_n}\tilde{V}_S(\mathbf{p},\mathbf{k},\omega_n-\nu_n)$$
$$\times[\nu_n^2+E(\mathbf{k},\nu_n)^2]^{-1}\phi(\mathbf{k},\nu_n)\,. \quad (4)$$

We have included only intraband pairing terms here, $E(\mathbf{k},\nu_n)$, and $u_\alpha(\mathbf{k})$ are the energy and wave function of

the conduction band, and ω_n, ν_n are fermion Matsubara frequencies. The singlet interaction $\tilde{V}_S$ is obtained from the effective interaction of Eq. (2):

$$\tilde{V}_S(\mathbf{p},\mathbf{k},\omega_n-\nu_n)=\sum_{ij}\tilde{g}^i(\mathbf{p},\mathbf{k})\tilde{g}^j(-\mathbf{k},-\mathbf{p}) \times[\Gamma_\rho^{ij}(p-k)-3\Gamma_s^{ij}(p-k)], \quad (5)$$

where

$$\tilde{g}^i(\mathbf{p},\mathbf{k})=\sum_{\alpha\beta} g^i_{\alpha\beta}(\mathbf{p},\mathbf{k})u_\alpha(\mathbf{p})u_\beta(\mathbf{k}).$$

We solve Eq. (4) by expanding the gap function $\phi(p)$ in square harmonics, keeping terms to second order (allowing up to second-neighbor correlations in real space). This allows for gap functions with A_{1g} ("extended s"), B_{1g} ($d_{x^2-y^2}$), or B_{2g} (d_{xy}) symmetry in the singlet channel. Equation (4) is most conveniently solved as an eigenvalue problem, being rewritten (in an obvious notation) as

$$[1-V\Pi]\phi=\lambda\phi, \quad (6)$$

with the transition temperature being defined by $\lambda(T_c)=0$.

We first present results for calculations using the bare Green's functions for quasiparticles. The dominant instabilities in the particle-hole channel are then either a SDW (for large U) or a CDW (for large V) with wave vectors near (π,π); both of these instabilities involve principally the Cu.[5] In Fig. 1 we show the results as a function of U and V at a hole concentration of $\delta=0.2$, with $\epsilon=0$, $t'=0.5$. In the figure, we mark all instabilities from the metallic state, although some of them will be preempted by other transitions. The superconducting transitions are indicated only when their transition temperatures T_c exceed $10^{-4}t$. As would be expected,[6] we find that a nearby antiferromagnetic instability (solid line) promotes d-wave (B_{1g}) and extended s-wave [A_{1g}, with a gap function principally[7] of the form $\cos(k_x a)+\cos(k_y a)$] superconductivity. We find that the transition temperatures for d-wave pairing are invariably higher in the vicinity of the SDW instability. Similar results for the single-band Hubbard model have been found by others.[8] In the vicinity of the CDW instability, we find a weak tendency for d_{xy} (B_{2g}) symmetry pairing, but the region where T_c exceeds $10^{-4}t$ is too narrow to display in the figure. Both B_{2g} and also an extended s-wave (A_{1g})[7] pairing instability with similar T_c are driven by the $q\sim 0$ charge-transfer resonance (CTR) of A_{1g} symmetry,[1] the mode which softens at the CTI. Of course, in Fig. 1, neither the CTI nor the associated superconductivity is accessible because they will be preempted by the CDW instability.

It was argued earlier[1] that the CDW instability is strongly suppressed by the inclusion of self-energy effects, and the dominant mode in the charge-fluctuation channel is then the $\mathbf{q}\sim 0$ CTR of A_{1g} symmetry. In Fig. 2 we show the results including self-energy corrections (to second order) for the quasiparticle propagators. For the calculations of superconductivity, we use a quasiparticle approximation (with effective-mass correction determined from the self-energy) while the full dynamical self-energy correction was included in the calculation of the particle-hole vertex of Γ. The results are qualitatively as found in Fig. 1 but with the suppression of the CDW instability; we find a sizable region of d-wave superconductivity at small V, and a narrow region of ex-

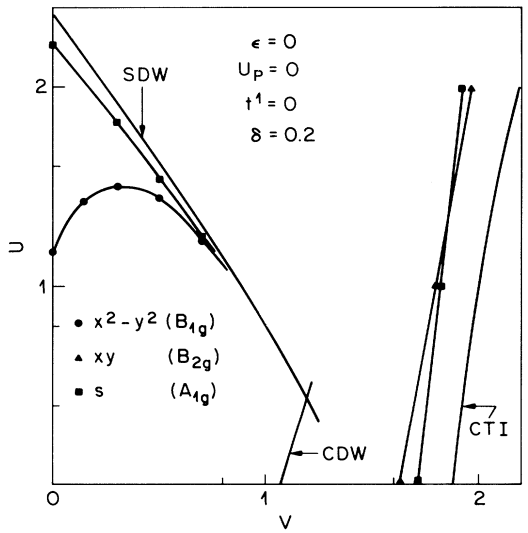

FIG. 1. Instabilities of the paramagnetic metallic state to either SDW, CDW, and CTI as well as the associated superconducting states, in a calculation neglecting self-energy corrections.

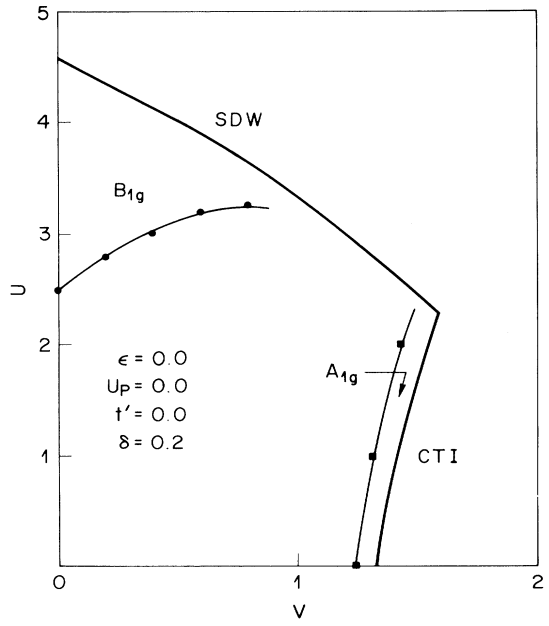

FIG. 2. Phase diagram as a function of U,V calculated for a hole doping of 0.2, including second-order self-energy corrections in the quasiparticle propagators.

tended s-wave superconductivity close to the CTI. The self-energy effects suppress the d_{xy} pairing in this case; although the results of Fig. 2 neglected O-O hybridization ($t'=0$) we have not found any strong influence of t' on the structure of the phase diagram (although the boundaries are of course shifted).

In Fig. 3 we plot the calculated superconducting transition temperatures for s-wave pairing as a function of doping, with (solid circles) or without (open circles) the inclusion of self-energy effects in the evaluation of Π [Eq. (6)]. In both cases, we used second-order self-energy corrections in the calculation of the interaction. In calculating the points in Fig. 3, we evaluated T_c at a fixed doping $\delta=0.2$ as a function of $V-V_c$, where V_c is the critical value of the intersite interaction for the CTI. Results at different dopings were obtained with the scaling assumption $T_c(\delta)=T_c(V_c(\delta)-V)$. Since the range of doping studied is quite small, this will be a good approximation; furthermore, it is less susceptible to delicate numerical errors than separate direct calculations at different fillings. The width of the superconducting regime as a function of doping is thus determined by the value of $\partial V_c/\partial\delta$ which in our calculations is small and negative, so that the region of superconductivity can be sizable. Similar results are obtained at different parameter values, provided only that they are such that the A_{1g} mode is soft.

In order to understand the details of superconductivity induced by charge fluctuations, it is convenient to study the effective interaction in real space. In Fig. 4 we plot the values of the effective real-space interactions (bare value given in parentheses) as a function of V in the vicinity of the CTI: Γ_{dd} (U), the effective copper U; Γ_{pp} (U_p), the same for oxygen orbitals; Γ_{pd} (V), the nearest-neighbor interaction between Cu and O; Γ_{xy} (zero), the interaction between nearest-neighbor O states. We see that the charge fluctuations provide attractive components to both the on-site interactions as well as the interaction between oxygen neighbors. However, the repulsion between quasiparticles on neighboring Cu and O atoms is *enhanced;* this effect largely counterbalances the attraction in other channels.

This result can be understood in terms of the polarization cloud for the A_{1g} CTR induced by a localized charge. A charge introduced onto an O site induces a polarization cloud which flows symmetrically from O to Cu; a second carrier will then see a deficit of charge (and hence be attracted) to the O site or O neighbors, and will experience a charge excess (and hence repulsion) on the Cu site. The same effect operates in reverse for a charge introduced first on Cu—in both cases, the mode promotes on site and O-O neighbor attraction but extra intersite repulsion. Unlike conventional phonon-driven superconductivity, in the present case, the repulsive and attractive channels have identical dynamics, so there are no prospects for reducing the repulsion by screening effects. Also, because the band structure *determines* the relative fraction of Cu and O states near the Fermi surface, it is not easy to avoid the repulsive interaction Γ_{pd} by constructing gap functions with nodes (as in the case of the Hubbard model) unless one admixes lower bands at a large price in kinetic energy. It is advantageous for the pairs to be confined to the O sites; this is promoted in the band structure by small ϵ and large t' and realized by the extended s character of the pairing. A sizable O-O overlap will tend to stabilize d_{xy} (B_{2g}) over extended s-wave pairing (A_{1g}); although this effect is weakened by self-energy corrections, we find that the two states are generally competitive in energy.

We have calculated the frequency dependence of the

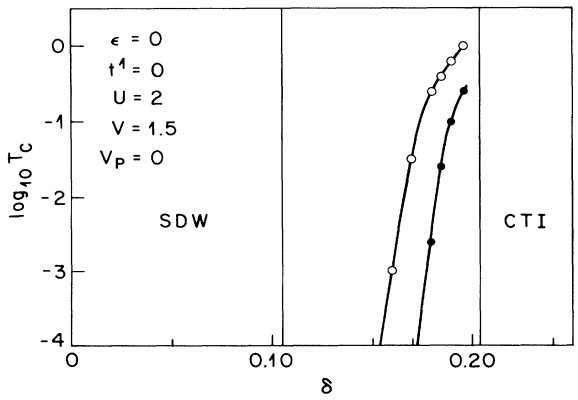

FIG. 3. Superconducting transition temperature T_c vs doping: with (solid circles) or without (open circles) effective-mass corrections.

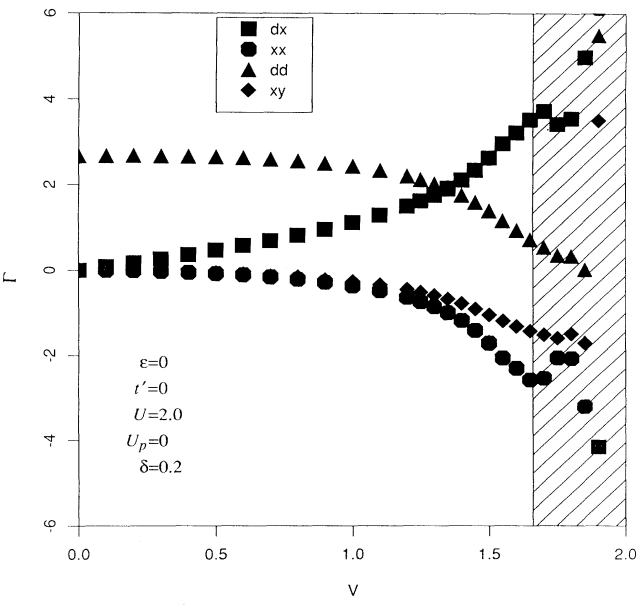

FIG. 4. Static ($\omega=0$) effective interaction in different channels as a function of V. The hatched region marks the CTI.

effective interactions Γ near the instability. The interaction does not have a strong frequency dependence, so we use the BCS approximation of treating it as frequency independent up to a cutoff. Calculations with the full dynamics of the interaction will be published separately.[9]

From Fig. 3, it appears that s-wave superconductivity with T_c in the range of $10^{-1}t$ is possible in the narrow composition region near the CT instability. In drawing conclusions regarding the Cu-O materials, the limitations (and strengths) of the weak-coupling methods should be kept in mind. We were forced to work with U/t not exceeding about 4 because for larger values the antiferromagnetic (AFM) instability prevails over a much wider range of composition in our approximation. It is generally accepted[10] that the on-site interactions U are larger than those employed here; in our calculation a larger U will suppress charge fluctuations and push the charge-transfer excitation to higher energies. Such a result is an artifact of the Hartree-Fock approximation, and the Hartree-Fock band structure is clearly defective in that it predicts too much Cu character at the Fermi level. Gutzwiller[11] or slave-boson[12] approximations do not have this shortcoming; with the same model they cease to give an AFM ground state for $\delta \gtrsim 0.05$ and $U/t \approx 6$. More sophisticated calculations of the overall charge density show a reduction of the relative Cu character at E_F, while charge fluctuations at low energy not involving double occupation of the Cu sites persist.[11] The value of T_c calculated here depends sensitively on the relative charge on Cu and on oxygen, and will change with the approximation used. The variation of T_c with composition depends on the details of the variation of the charge-fluctuation spectrum with composition. In better approximations, this will be smoother than calculated here, and so will be the T_c.

We do expect, however, that the general qualitative features calculated in the generalized random-phase approximation are correct. We find that the metallic phase exists only for a limited range of composition bounded on one side by the AFM instability and on the other by the CTI. Although we have presented data here only for $\epsilon = U_p = 0$, we have found that the structure of the phase diagram is not changed for different parameter values, although the positions of the phase boundaries are moved. In particular, increasing ϵ favors antiferromagnetism at smaller U_d, and increasing U_p or U_d pushes the CTI to larger values of V; the effect of U_p is much weaker than U_d because there are twice as many O sites and the hole double occupancy on oxygen is small. However, in all cases we find near the CTI a region of s-wave superconductivity with significant T_c; near the SDW, d-wave pairing is stable.

For a given set of bare parameters there are two self-consistent (Hartree-Fock) values of ϵ beyond the CTI with a critical point at $\epsilon = 0$. They correspond to different sets of Cu-O charges, typically differing by (10–20)%. The CTI signals this charge-disproportionation instability among different unit cells and is in accord with the inability to dope these materials (and maintain a homogeneous phase) beyond a critical concentration. Our calculations at $\epsilon \sim 0$ make use of the fluctuations near this instability for superconductivity. Note that the A_{1g} CTR couples to phonons of the same symmetry; there are no such modes for a single layer (except uniform compression), but a coupling to out-of-plane vibrations, particularly of the O(4) atom, is expected.

The CTR is not found in the one-band Hubbard model, or a multiband model without charge-transfer fluctuations driven by interatomic repulsion terms in Eq. (1). These terms represent the Madelung energy of these ionic solids, and play a dynamical role when $|E_d - E_p| \ll 4t$. We have shown that these modes do promote s-wave superconductivity, leading to a phase diagram whose general features are found in the real materials.

We wish to thank Stefan Schmitt-Rink and Sue Coppersmith for discussions.

[1]P. B. Littlewood, C. M. Varma, S. Schmitt-Rink, and E. Abrahams, Phys. Rev. B **39**, 12371 (1989).

[2]C. M. Varma, S. Schmitt-Rink, and E. Abrahams, Solid State Commun. **62**, 681 (1987); and in *Novel Mechanisms of Superconductivity,* edited by V. Kresin and S. Wolf (Plenum, New York, 1987), p. 355.

[3]E. R. Gagliano *et al.*, Solid State Commun. **64**, 901 (1987); C. A. Balseiro *et al.*, Phys. Rev. B **38**, 9315 (1988); J. E. Hirsch *et al.*, Phys. Rev. Lett. **60**, 1668 (1988); C. A. Balseiro *et al.*, Phys. Rev. Lett. **62**, 2624 (1989); M. D. Nunez Regueiro and A. Aligia, Phys. Rev. Lett. **61**, 1889 (1988); S. Trugman (to be published); Z. Tesanovic, Bull. Am. Phys. Soc. **34**, 714 (1989).

[4]W. R. Hanke and L. J. Sham, Phys. Rev. B **12**, 4501 (1975); S. K. Sinha, R. P. Gupta, and D. L. Price, Phys. Rev. B **9**, 2564 (1974).

[5]Since the direct Coulomb interaction vanishes near the nesting wave vector [$\sim(\pi,\pi)$ near half filling], the CDW instability is driven by the Cu-O exchange interaction. In contrast, the CTI involves charge transfer between Cu and O and is driven by the direct Cu-O interaction V.

[6]See, e.g., K. Miyake, S. Schmitt-Rink, and C. M. Varma, Phys. Rev. B **34**, 6554 (1986).

[7]There is of course mixing with the on-site s wave, but we find that this component is typically $\lesssim 10\%$ of the "extended" s, near both the SDW and the CTI boundaries.

[8]D. J. Scalapino, E. Loh, and J. E. Hirsch, Phys. Rev. B **34**, 8190 (1986); G. Bickers *et al.* (to be published).

[9]J. Bang, K. Quader, E. Abrahams, and P. B. Littlewood (to be published).

[10]Calculated values for the three-band Hubbard model give the approximate values $U_d/t = 8$, $U_p/t = 3$, $V/t = 1$, $t'/t = 1/2$, and $\epsilon \sim 0$, the latter implying a *bare* $\epsilon \sim 3t$; see M. S. Hybertsen, M. Schluter, and N. E. Christiansen, Phys. Rev. B **39**, 9028 (1989); A. K. McMahan, R. M. Martin, and S. Satpathy, Phys. Rev. B **38**, 6650 (1988).

[11]S. N. Coppersmith (to be published); S. N. Coppersmith and P. B. Littlewood (unpublished).

[12]C. A. Balseiro *et al.*, Phys. Rev. Lett. **62**, 2624 (1989).